MODELING THE SPATIAL DISTRIBUTION OF LIGHTNING FIRES ON TWO NATIONAL FORESTS

BY

SARA H. BROWN

A thesis submitted in partial fulfillment of
the requirements for the degree of

MASTER OF SCIENCE IN ENVIRONMENTAL SCIENCE

WASHINGTON STATE UNIVERSITY
School of Earth and Environmental Sciences

AUGUST 2009

To the Faculty of Washington State University:

The members of the Committee appointed to examine the thesis of SARA H. BROWN find it satisfactory and recommend that it be accepted.

_____
Richard Gill, Ph.D., Chair

_____
Robin Reich, Ph.D.

_____
Matt Carroll, Ph.D.

ACKNOWLEDGMENT

I would like to acknowledge my family and academic committee members for their support in assisting me complete this thesis.

MODELING THE SPATIAL DISTRIBUTION OF LIGHTNING FIRES ON TWO NATIONAL FORESTS

Abstract

by Sara H. Brown, M.S.
Washington State University
August 2009

Chair: Richard Gill

Forest fire ignitions on National forest lands have many causes; however lightning remains the most consistent ignition source. By understanding the spatial distribution of lightning fires over a sixty-five year temporal scale allows fire and timber managers to gain a better understanding of how to spatially locate, and manage, fuel treatments on these forests. It is hypothesized that elevation plays a significant role in the probability of a lightning strike igniting a forest fire given acceptable climatic and fuel conditions. The two study areas were chosen for several reasons; first, fire suppression data was available across a similar temporal scale for both forests. Second, the Gallatin National Forest in Montana provides a platform to test this hypothesis in a *Pinus contorta* dominated, high severity fire regime, while the Willamette National Forest in Oregon provides a mixed-conifer mixed severity fire regime. Additionally, these two forest types provide over two million acres upon which to test our point process model. An inhomogeneous Poisson cluster point process model was developed to describe the spatial distribution of lightning-caused fires as a function of elevation on the Gallatin and Willamette National Forests. The results of this study provide a range of elevations at which the probability of a lightning strike igniting a forest fire is significantly higher on

each forest. On the Willamette National Forest, elevations between 700m and 1600m have the highest ignition probability, while the Gallatin National Forest high probability elevations ranged between 2300m to 2600m. Managers of these two forests, as well as managers of similar forest types, can focus attention at these elevations for both fuel reduction efforts as well as urban interface fire suppression efforts.

TABLE OF CONTENTS

LIST OF TABLES

LIST OF FIGURES

Dedication

This thesis is dedicated to firefighters past, present, and future.

INTRODUCTION

Fire is a widely recognized ecological driver and an important part of the disturbance regime of the western United States. Scarcity of fires during the 20th century in some ecosystems may be the result of successful fire suppression policies. However, the past ten years has seen an average increase of 10% per year in land area consumed by wildfire as compared with the previous decade (National Interagency Fire Center, 2008). With more complete modern records, and an increase in land under federal protection since the 1960's this trend is unmistakably apparent over the past half-century (Schoennagel et.al., 2004). In 2000, for example, over 3.5 million ha burned in western Montana, northern Idaho, and California despite over $1.3 billion spent on fire fighting efforts (National Interagency Fire Center, 2008). Additionally, 1998 and 2002 burned 3.0 million and 2.8 million ha respectively; the year 2006 has proven to be one of the largest fire years, with over 3.8 million ha burned and $875 million spent on suppression (National Interagency Fire Center, 2008).

The role of fire as important ecological process on the landscape has become well understood in both the scientific and management communities over the past several decades. A greater management emphasis on the use of controlled fire on public lands increased in the mid-1980s with a focus on managing natural fuel buildup that has occurred over several decades of successful fire suppression and other stringent fire control policies. Recent large fire events have been widely blamed on fuel build-up, in particular the "thickening" of the forest that has occurred in recent decades in the absence

of fire and harvest. This idea was developed primarily from experience in dry ponderosa pine (*Pinus ponderosa*) forests in the US Southwest, the interior West and the Sierra Nevada, rather than in wetter forests where the absence of fire is consistent with long-term fire regime patterns (Covington and Moore, 1999).

As a blanket approach to this "fuel build-up" problem, the National Fire Plan directed over $200 million be allocated in 2001 as part of a fuel mitigation program, and increased suppression effort (USDA Forest Service, 2002). In 2002, thinning and prescribed fire projects were carried out across 1 million ha of federal land (www.fireplan.gov, 2009) to reduce the fire hazard and to restore historical species composition and stand structure. The goals of this fire hazard reduction and ecological restoration may converge in some ecosystems, yet they may be incompatible in others (Veblen et al., 2000). Nonetheless, managers of federal forests have focused much of their attention on trying to identify and recreate the fire regimes that existed at the time of Euro-American settlement and before extensive fire suppression was in existence.

Packaged in this ecological framework, the ultimate target of these mandated fuel management activities is to reduce the damaging effects of large fires on human communities, as well as provide fiscal relief to tax payers from the exponential increase of fire suppression costs. While these targets also include ecological considerations such as fire damage to soils and rare and endemic species, a balance must be reached. The ecological damage to the White Mountain Apache Reservation in Arizona after the Rodeo-Chediski Fire in 2002 was unprecedented. That same year similar impacts from

the catastrophic Hayman Fire in Colorado were seen in riparian areas and surrounding soils (NIFC, 2008) (Shoennagle et.al, 2004). True ecological stability of forested areas requires fire to burn naturally; unsuppressed over large, and small, forested areas at a variety of intensities. Obviously fire suppression is a social necessity at this time.

One of the variables that forest and fire mangers have struggled with for the past century is spatially locating and accessing fire starts. Numerous location tactics have been used on National forests throughout fire suppression history: Fire lookouts on high peaks, patrols throughout forested areas (on foot and in vehicles), air patrols in fixed wing and rotor-wing aircraft, and more recently, online real-time atmospheric lightning maps. Each of these methods have benefits, however each faces the same weakness--a long time lag from time of fire ignition to full suppression. Once a fire location has been identified, fire managers must determine how to get suppression professionals to the fire in a timely manner. Ground crews can travel by vehicle to get as close to the fire incident as possible, then continue on foot to suppress it. Fire engines require the same vehicular drive time getting to the incident. Helicopters have a shorter travel time to the fire, but require either a large landing site, or a safe rappel site to get troops to the fire. Fixed wing aircraft can drop personnel via parachute relatively close to the fire, but personnel usually must hike on foot to the fire once arriving on the ground. Each of these delivery methods requires a significant amount of time. Under hot, dry conditions in dense fuels, fires can burn large areas in short periods of time (Shoennagle et.al., 2004). These conditions allow fires to escape control of the suppression experts before they even arrive at the fire scene.

Lightning is a leading natural cause of wildfire ignitions. In the Intermountain West, lightning accounts for a high proportion of forest fires that cause substantial damage (Borig and Ferguson, 2002). Lightning fires burn a disproportionate share of National forest land because they are harder to detect and reach, and they arrive in spatial and temporal clusters that can strain fire managers. Because of this important contribution to the total number of fires and area burned, research in this area has been a priority since organized fire protection began (Podur et.al., 2003). Gaining insight into the spatial distribution of lightning fires allows predictions to be made about general areas within a given landscape that will receive a high number of ignitions.

If managers had the ability to predict general areas where fires were likely to start, several protocols could be put in place that would drastically reduce the amount of time necessary for personnel to start active suppression, or suggest "let it burn" protocol. Fire engines and crews could be staged in the predicted area. Forest fuel treatments could be completed in these specific areas rather than on a landscape scale, saving significant time and money; and urban interface areas could be prepared for imminent fire danger.

In this paper, the spatial distribution of lightning caused fires on two national forests, the Willamette in Oregon, and the Gallatin in Montana will be examined. These two forests provide both dry and wet forest environments, as well as have varying degrees of harvest and fuel treatments practiced over the past 50 years. It is hypothesized that the spatial distribution of lightning caused fires reflects an underlying spatial variation in the

environment with respect to its suitability to ignite a fire. Elevation can influence the probability of lightning strikes, and given the right conditions, the likelihood of a fire (Granstrun, 1993; Marsden, 1982). Modeling the spatial distribution of lightning fires as a function of elevation on a given National forest will provide an approximate elevational band for forest and fire managers to target. Suppression personnel staging, fuel treatments, and creating defensible space around urban interface areas can be done with the target elevational bands in mind. Limiting these efforts to an elevational "band" within the National Forest will save time, money and theoretically lead to fewer large uncontrolled fires.

This study uses historical fire suppression records from both the Willamette National Forest in Oregon, and the Gallatin National Forest in Montana to provide fire locations over a 65 year period from the year 1940 to 2005. A single fire event has been recorded throughout US history as a point-based concept, described by its x and y geographic position, rather than an area based event. It has only been in the past few decades that accurate spatial estimates of fire, as well as the surface nature and spreading behavior of a fire have been recorded. Using the spatial fire data available, a parsimonious inhomogeneous Poisson cluster process model is used to model the spatial distribution of lightning fires on these two National Forests.

METHODS

Study Site Description

The two research sites are the Willamette National Forest in Oregon, and the Gallatin National Forest in Montana. When added together, both forests total over 1,375,931 ha in size. Basic climate, elevation, vegetation, and forest history information further describe the important ecological differences between these two forest types. Determining how elevation impacts fire ignitions in these two divergent fire regimes will provide managers locations to target during fire suppression, staging and fuel management.

Willamette National Forest

The Willamette National Forest (Figure 1) was originally established in 1893, and was administratively organized in its current form as a National Forest in 1933. It has been managed by the Forest Service within the U.S. Department of Agriculture since 1905. About one-fifth of the forest (154,106 ha) is designated as wilderness (USDA Forest Service, 2008).

The Forest is 678,013 ha in size and stretches for 110 miles along the western slopes of the Cascade Range in western Oregon. It extends from the Mt. Jefferson area east of Salem, to the Calapooya Mountains northeast of Roseburg. Elevations on the forest range from 1,500 feet (457.2 m) above sea level to 10,495 feet (3198.8 m) atop Mt. Jefferson, Oregon's second highest peak. The Forest receives a large amount of precipitation each year, much of it as snow from October through April (USDA Forest Service, 2008).

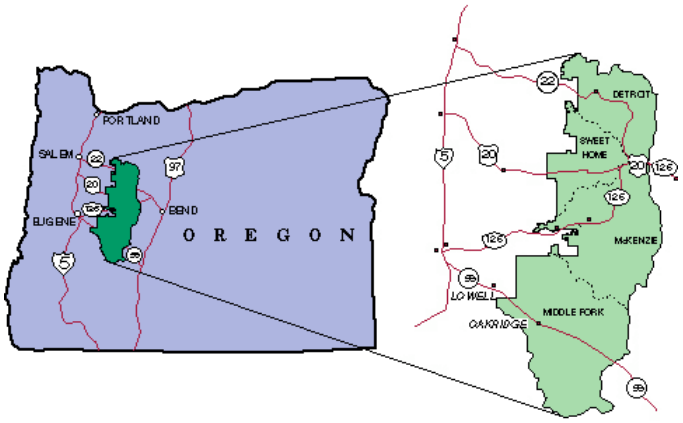

Figure 1: Location of the Willamette National Forest. (USDA Forest Service, 2008)

The landscape is varied; most of the forest is covered with Douglas-fir (*Pseudotsuga menziessi*), a valuable timber species in the United States. At least 15 other conifer species are also common on the forest, these species are combined into four basic forest types. Douglas-fir is the most common. Second dominant is mixed conifer. Third is Pacific silver fir, and fourth is mountain hemlock (Table 1), (USDA Forest Service, 2008).

Table 1: Four most common forest types in rank order on the Willamette National Forest.

Forest Type	Major Tree Species within Forest Type
1. Douglas-fir	Douglas-fir (*Pseudotsuga menziessi*), western hemlock (*Tsuga heterophylla*), western redcedar (*Thuja plicata*)
2. Mixed conifer	Douglas-fir (*Pseudotsuga menziessi*), grand fir (*abies grandis*), sugar pine (*Pinus lambertiana*), incense cedar (*Calocedrus decurrens*), ponderosa pine (*Pinus ponderosa*).
3. Pacific Silver fir	Hemlock (*Tsuga Canadensis),* Pacific silver fir (*Abies amabilis*)
4. Mountain hemlock	Mountain hemlock (*Tsuga mertensiana)*

While many consider the western Cascade Mountains to be wet, the climate in the Pacific Northwest can be very dry during the late summer and early fall. This climate regime and the flammable nature of coniferous tree needles and branches combine to produce an ecosystem that is subject to and adapted to wildfire. Depending upon forest conditions, the time of year, and local weather, fires can be slow creeping ground fires that reduce the amount of flammable fuel on the forest floor, (while killing most of the understory vegetation), or they can be crown fires that may kill tens of thousands of acres of trees (USDA Forest Service, 2008). Under this fire regime, fires are fairly frequent, but of relatively low intensity. Most fires occur between the months of June and October.

The diverse landscape is known for historically yielding a sustainable supply of timber and special forest products. Old growth was preferentially harvested on the forest from the mid 1920's to the early 1980's. During WW II, the Willamette increased timber sales to provide resources for the war effort. Between 1942 and 1945, the Willamette sold 559 million board feet (MMBF) of timber. The years 1945 to 1970 mark an era of intensive forestry and forest management. This era included dramatic increases in recreation use, timber sales, dam construction, campground construction, and wildlife management. The passage of the Wilderness Act (1964) created new wilderness areas and controversy over the management of the new areas. This era also marked the establishment and growth of an activist environmental movement. Today less than 50 MMBF are removed from the forest (USDA Forest Service, 2008).

Gallatin National Forest

The Gallatin National Forest (Figure 2) was established in 1899. Today, the Gallatin is part of the Greater Yellowstone Area, the largest intact ecosystem in the continental United States. The 728,434 ha forest spans six mountain ranges and includes two congressionally-designated wilderness/roadless areas totaling 625,425 ha. Elevations range from 5,000-11,000 feet (1524m-3352m) (USDA Forest Service, 2008).

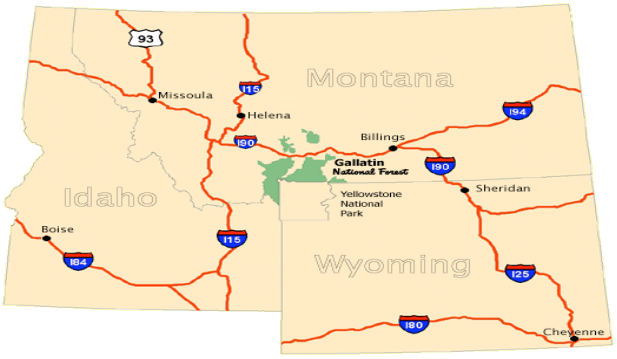

Figure 2: Location of the Gallatin National Forest (in green) (USDA Forest Service, 2008)

Grass and shrub habitats occupy the drier south and west-facing slopes throughout the forest. Along with the grass/shrub habitats, pure Douglas-fir (*Pseudotsuga menziesii*) forests also occupy the drier south and west-facing slopes. The north and east-facing slopes throughout the forest consist of a mix of Douglas-fir /lodgepole pine (*Pinus contorta*) or Douglas-fir/lodgepole pine/subalpine fir (*Abies balsamea*) forests. These stands characteristically consist of dense tree canopy cover, abundant understory vegetation and moderate to high levels of downed fuel. Scattered groves and individual aspen (*Populus spp.*) trees are found throughout the forest as well.

Fires are particularly important to regeneration and survival of high elevation whitebark (*Pinus albicaulis*) pine on the forest. This pine species often survives low-intensity surface fires, which more easily kill associated conifers (Morgan et. al., 1992). Stand-replacing fires also benefit whitebark pine, although all trees are usually killed. Whitebark pine regenerates on burned sites more successfully than many associated tree species (Tomback et. al., 1990). Since the onset of successful fire suppression in the early 1940's, fewer fires have occurred in the subalpine and timberline environments, contributing to declining abundance of whitebark pine (Morgan et. al., 1992). In the absence of fire or other major disturbances, whitebark pine is replaced by subalpine fir on most of the higher elevation landscapes.

Before the 1950's much of the harvest on the Gallatin was for railroad ties, mine timbers, posts and poles, lumber and firewood. Various methods were used to complete the harvest (hand, horse and mechanical). Clearcutting became a primary method of harvest

in the accessible areas across the forest. Approximately 2.5 MMBF of timber was harvested from 1961 to 1970. Beginning in the early 1970s to the mid-1980s, an epidemic of mountain pine beetle mortality resulted in a significant amount of timber harvest activity across the forest. Mechanical clear-cut harvest was intense through this period as the forest dealt with the mountain pine beetle epidemic. Many of the early (1950 – 1980) harvest treatments have since regenerated and been pre-commercially thinned to improve growth, form, vigor and reduce insect and disease problems (USDA Forest Service, 2008).

Spatial Analysis

All data for this project was gathered from the USDA Forest Service. Digital elevation models (DEM) and forest boundary data were provided via geographic information systems (GIS) for each forest. Historical fire suppression records from the earliest date recorded (1940) through 2005 were obtained from both National Forests as well. Fire suppression records provided information including size of fire, start date, cause, and suppression efforts.

The fire data for each forest were entered into an Excel database, to create histograms of the causes of the fires. It was determined that lightning fires constituted a significant proportion of the total number of fires. All lightning fires were then selected for analysis. Each of the lightning fire locations over the entire temporal scale of 65 years were imported to a GIS layer using universal transverse mercator (UTM) coordinates for each forest.

To describe the spatial distribution of lightning-caused fires, large rectangular regions were selected within each National forest. Because of the shape of the Willamette, two rectangular areas were necessary to capture the majority of fire clusters; on the Gallatin only one large area was necessary (Figures 3 and 4). The rectangular regions were selected to simplify the algorithm required to adjust for edge effects, and to include as many fires as possible to represent the spatial relationship between lightning-caused fire and elevations throughout each forest. Figures 5 and 6 depict the spatial location of all fires during the study period overlaid on the DEM of each forest

All spatial analysis was based on Ripley's k-function (Ripley 1977). Ripley's k-function is a second-order neighborhood analysis developed to test various hypotheses regarding the spatial distribution of mapped data sets by examining the proportion of total possible pairs of points in Euclidean space whose pair members are within a specified distance of each other. The analysis is a second-order because it is based on the variation rather than the mean of distances being studied.

Ripley's k-function is the cumulative distribution function of distances from points in a region A to other points in A:

$$\hat{F}(d) = \frac{\sum_{i \neq j} I_{ij}(d)}{N(N-1)} \qquad (1)$$

where $I_{ij}(d) = 1$ if the distance, d_{ij}, between points i and j are less than some specified distance, d, and 0 otherwise, and N is the total number of points in the population. The

function *F(d),* will be subject to a downward bias if no allowance is made for boundaries. To take into consideration edge effect Ripley replaces *F(d)* with

$$\hat{K}(d) = \frac{A\sum K(i,j)}{N(N-1)}. \qquad (2)$$

For a Poisson process $\hat{L}(d)$ has an approximate mean of *d*, and approximate variance of $1/(2\pi N^2)$. For a unit square, $\hat{L}(d)$ is an estimate of the proportion of the population within *d* units.

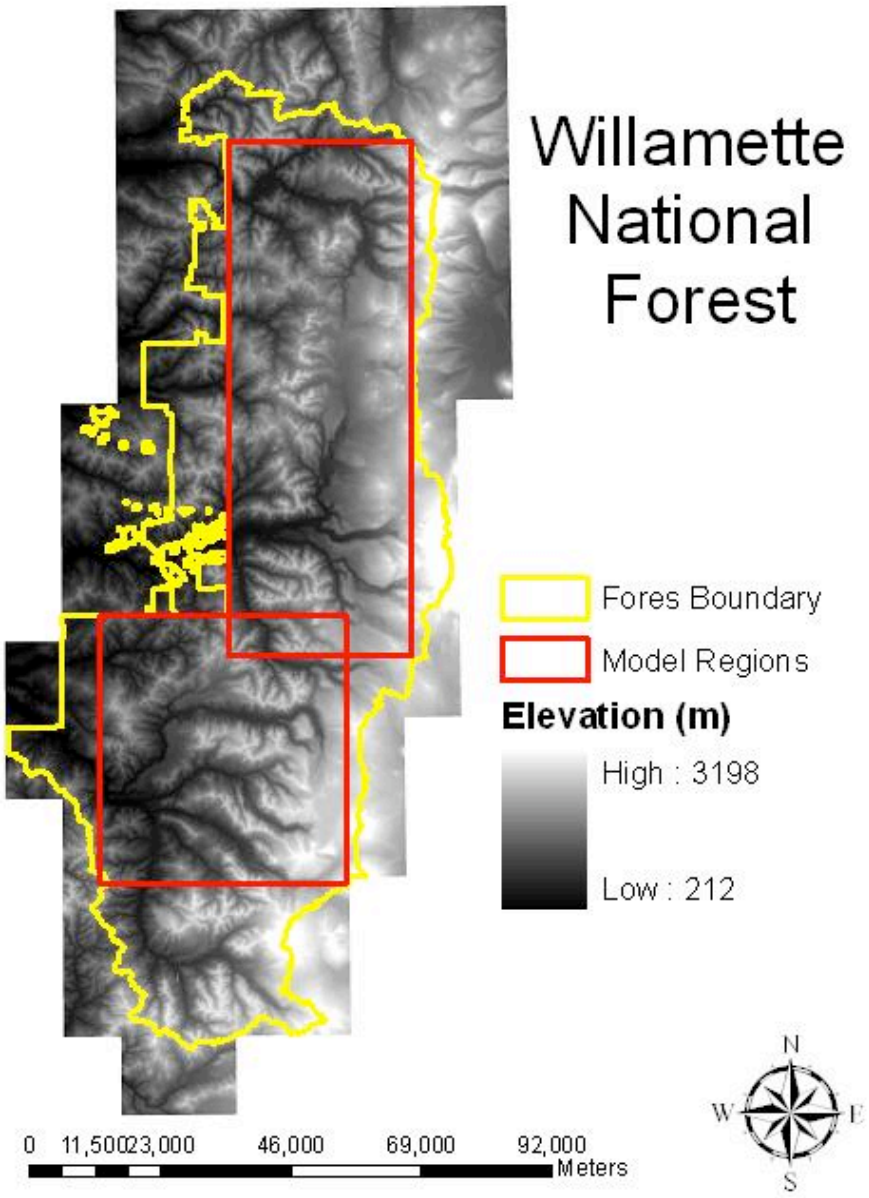

Figure 3: DEM of the Willamette National Forest. The yellow line depicts the National Forest boundary. The red rectangle depicts the sub-region used to evaluate the spatial distribution of lightning-caused fires.

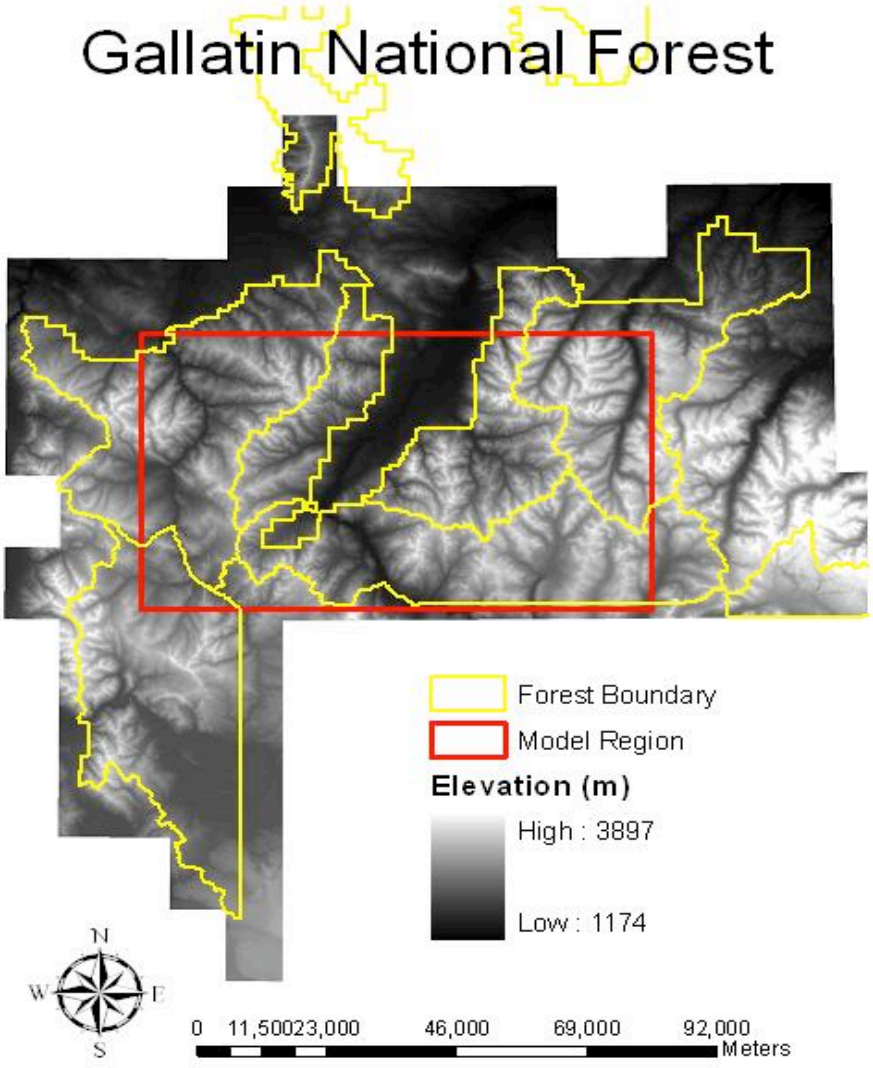

Figure 4: DEM of the Gallatin National Forest. The yellow line depicts the National Forest boundary. The red rectangle depicts the sub-region used to evaluate the spatial distribution of lightning-caused fires.

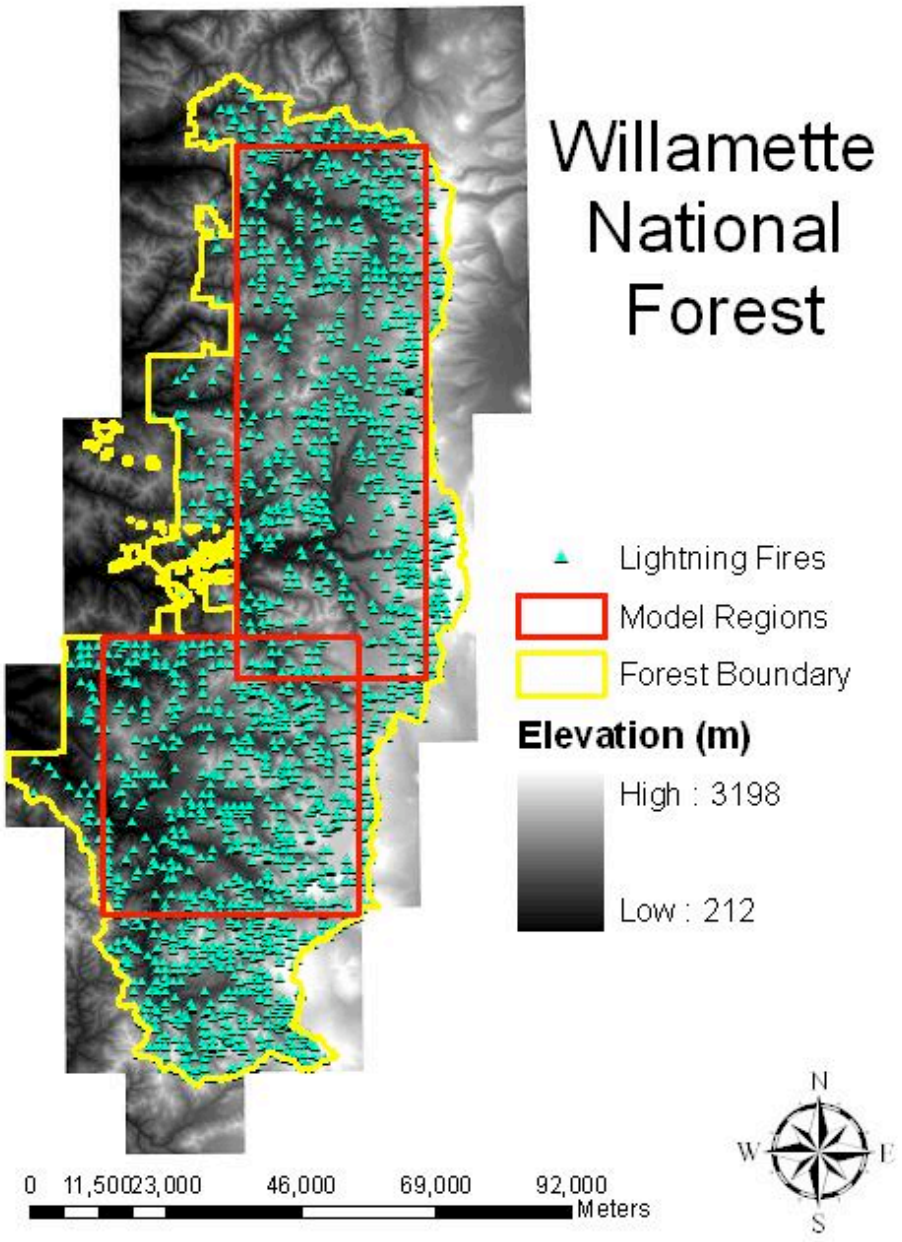

Figure 5: DEM of the Willamette National Forest overlaid with locations of all lightning fires (teal dots) during the years 1940-2005. The red rectangular region designates the sub-region used to evaluate the spatial distribution of lightning caused fires.

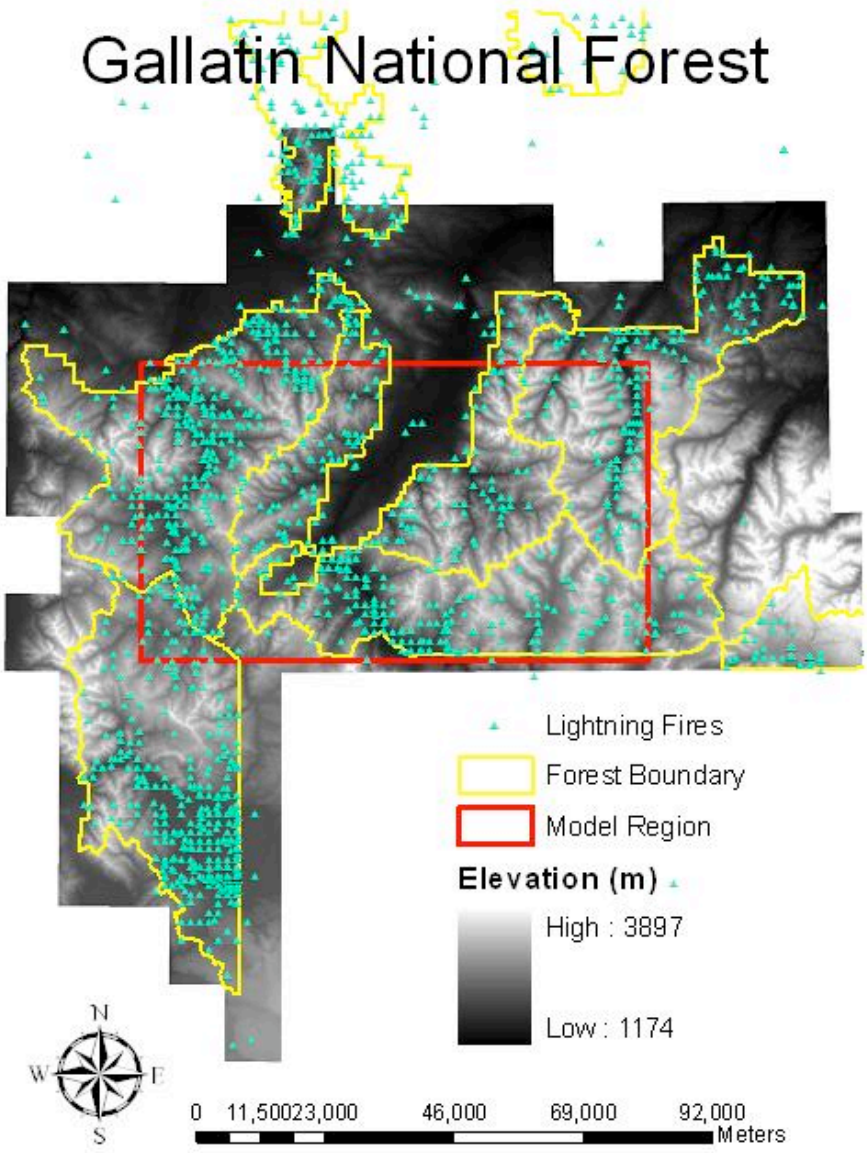

Figure 6: DEM of the Gallatin National Forest overlaid with the location of all lightning fires (teal dots) during the years 1940-2005. The red rectangular region designates the sub-region used to evaluate the spatial distribution of lightning caused fires.

Test for Complete Spatial Randomness

The first step in the analysis was to test the null hypothesis; that lightning caused fires are randomly distributed. Using the spatial location of each lightning-caused fire in the rectangular regions, a Monte Carlo test (Besag and Diggle, 1977) based on the Cramér-von Mises type statistic (Cressie, 1991)

$$k = \int_0^H \left\{ \hat{K}(h)^{1/2} - \pi^{1/2} h \right\}^2 dh \qquad (3)$$

was used to test the null hypothesis of complete spatial randomness (csr); where $\hat{K}(h)$ is the empirical k-function evaluated at distance h. For a Poisson process, the expectation is of $\hat{K}(d) = \pi d^2$. To apply this test we first calculate k_1 from the data. Next, k_i, $i = 2, \ldots, R$ are calculated as a realization of a Poisson process. Next, we rank the k_i's from1 to R where r is the rank of k_1. The significance level of the test statistic was calculated as: $\hat{p} = (R + 1 - r)/R$. If $\hat{p}$ is small we would reject the null hypothesis of *csr.* A small k_1 supports the null hypothesis. All tests were based on 150 realizations of a spatial Poisson process to allow for the calculation of a p-value to the nearest 1 percent.

Modeling the Probability of Lightning-Caused Fires

If the null hypothesis of complete spatial randomness was rejected, the next step in the analysis was to model the relationship between the spatial distribution of lightning-caused fires and elevation. It was assumed that some elevations, E, had a higher probability of a lightning fire than other elevations. Information was available for lightning strikes that started a fire, while no information was available on the location of strikes that did not start fires, or fires that died out soon after ignition (Podur et. al., 2003*;*

Larjauaara et. al., 2005). Thus, it was not possible to find the exact relationship between lightning caused fires, elevation and other variables, but only whether certain elevations had a higher or lower likelihood of lightning caused fires.

Let $Y_i = 1$ if a lightning fire occurs at elevation X_i, and $Y_i = 0$ if there is no fire:

$$Y_i = 1 \quad \text{when} \quad E_i \le X_i$$
$$Y_i = 0 \quad \text{when} \quad E_i > X_i$$

For a given elevation X_i selected at random

$$P(Y_i = 1 \mid X_i) = P(E_i \le X_i) \tag{4}$$

the probability $P(E_i \le X_i)$ is the cumulative probability distribution function (cdf) of lightning fires across all elevations in a given National forest. If the cdf of lightning caused fires is logistic:

$$cdf = \frac{\exp(y)}{(1 + \exp(y))} \tag{5}$$

where

$$y = \ln\left(\frac{\pi_i}{1 - \pi_i}\right) = \hat{\beta}_0 + \hat{\beta}_1 x_1 + \ldots + \hat{\beta}_k x_k \tag{6}$$

π_i is the cumulative probability associated with the *i*th fire. A general linear model (GLM) (Neter et. al., 1985) was used to fit a polynomial regression to describe the relationship between the logit transformation (y) and elevation
(E) (Appendix A). The Y_i's maximum likelihood estimates of the β_i's were obtained using R, (2005).

Taking the first derivative of $P(E_i \le X_i)$ yields the probability density function of lightning caused fires, $p(x)$.

$$p(x) = \frac{y'\exp(y)}{(1+\exp(y))^2}. \qquad (7)$$

where y' represents the first derivative of y with respect to elevation.

Parameter Estimation, Fitting the Model

Specific elevation values were derived for the location of all lightning-caused fires from the DEM's of each forest. This information was then used to develop a probability model describing the relationship between the presence of a lightning-caused fire, and elevation. The logistic response function was assumed to be an appropriate descriptor of the relationship between lightning-caused fires and elevation. The empirical distribution function was used to approximate the cdf, which concentrates probability 1/n at each of the n lightning-caused fires in the dataset. The empirical distribution function $F_n(X_i)$ based on a sample $X_1, \ldots, X_n$ is a step function defined by

$$F_n(X) = \frac{\text{Number of elevations in the sample} \le X}{n} = \frac{1}{n}\sum_{i=1}^{n} I(E_i \le X) \qquad (8)$$

where $I(A)$ is an indicator function.

Polynomial logistic regression was used to describe the cdf of the probability of a lightning-caused fire and elevation. Model parameters were estimated using maximum likelihood methods. First, the equation was fit using a first-order (linear) model. Then

additional parameters were added until they did not substantially add to the fit. Model and predictor significance were obtained from the Wald test statistic assuming a chi-square distribution with 1 degree of freedom (Harrell, 2001). The relative fit of each model to the data was evaluated using Akaike Information Criteria (AIC, Akaike, 1978). The selected model was used in conjunction with the DEM to create a GIS grid of the probability of lightning-caused fires for the two National forests.

Modeling Spatial Clustering

Visual observations of the spatial distribution of lightning fires suggest the possibility of clustering. If the null hypothesis of csr was rejected and it was not possible to model the spatial distribution of lightning caused fires as a function of elevation, the point data was fit to a Neyman-Scott point process model. The k-function for a Neyman-Scott point process is given by (Cressie, 1991):

$$K(h;\sigma^2, \rho) = \pi h^2 + \rho^{-1} \{1 - \exp(-h^2/2\sigma^2)\} \qquad (9)$$

where ρ is the intensity of the clusters which is assumed to be a homogeneous Poisson process, and $2\sigma^2$ is the mean squared distance to a lightning caused fire from the cluster center. The first term in Eq. 9 represents a Poisson process while the second term assumes a random number of fires per cluster positioned in a radially symmetric (Gaussian) way around the cluster center. The extent of clustering is given by:

$$K(h;\sigma^2,\rho) - \pi h^2 . \qquad (10)$$

Next, let K(h; θ) denote a model for the K-function and let $\hat{K}(h)$ be a nonparametric estimator obtained from the data. A non-linear least-squares estimator for θ was obtained by minimizing the ad hoc criteria:

$$D(\theta(= \int_0^{h_0} \left\{ \hat{K}(h))^c - (K(h;\theta))^c \right\}^2 dh \qquad (11)$$

where h_0 is the range in which the model is being fitted and c is a tuning constant. The power transformation parameter c is used to control for heterogeneity of variance of the estimate $\hat{K}(h)$. For a Neyman-Scott process it is recommended to use c = 0.25.

Simulation

The spatial distribution of lightning caused fires was simulated using the Lewis and Sholders (1979) rejection sampling algorithm. Let $p_{max} \equiv \sup p(x)$, where $p(x)$ is the probability of observing a lightning-caused fire. First, simulate a homogeneous Poisson process over the region B, with intensity $N(B)p_{max}$, where N(B) is the number of lightning caused fires in the region B. A lightning caused fire is retained with probability $p(x)/p_{max}$. For a Neyman-Scott process, cluster centers were distributed as an inhomogeneous Poisson process. Lightning fires were assigned to randomly selected clusters. The location of the fire relative to the cluster center has distribution h (x,y) and is retained with probability $p(x)/p_{max}$.

The goodness-of-fit of the point process model was assessed by comparing the transformed empirical k-function ($\hat{L}(h) = \left\{\hat{K}(h)/\pi\right\}^{1/2}$) (Ripley, 1977), corrected for edge effect (Cressie, 1991), to the transformed k-functions from 150 simulated realizations of the model. The simulations were used in constructing simulation envelopes based on the minimum and maximum transformed k-function to test the null hypothesis of no significant differences at the $\alpha = 0.007$ level. If, for any distance, the observed transformed k-function falls above or below the simulation envelopes the null hypothesis is rejected at the appropriate level of significance.

To evaluate the various models, a Cramer von-Mises type statistic was calculated. The proportion change in the statistic relative to the null model of complete spatial randomness was used as a measure of the overall fit of a model. A value near 0 would indicate no improvement over the null model of complete spatial randomness, while a value near 1 would indicate an exact fit.

RESULTS

Lightning ignitions on the Willamette National Forest account for 54% of all fires (N= 6,031 fires) over the 65-year study period (Figure 7). Other leading causes of ignition on the forest were campfire and smoking (cigarettes, lighters) (Figure 8). The size-class of the fires ranges from .0008 to over 424 hectares. The most common size ranges from .0008-0.09 hectares (Figure 9). On the Gallatin National Forest, lightning ignitions accounted for 50% of the total number of fires (N=2,023 fires) (Figure 10). Other leading causes of ignition on the forest were campfires, smoking, and "other," (Figure 11). The

fire size-classes range from .04 to 7475 hectares, with the most common size-class at approximately .5 hectares (Figure 12). Fires can occur on both forests at any time throughout a given year, however the highest frequency is during summer months. Lightning-caused fires are typically limited to the months March through October, with July and August having the highest frequency.

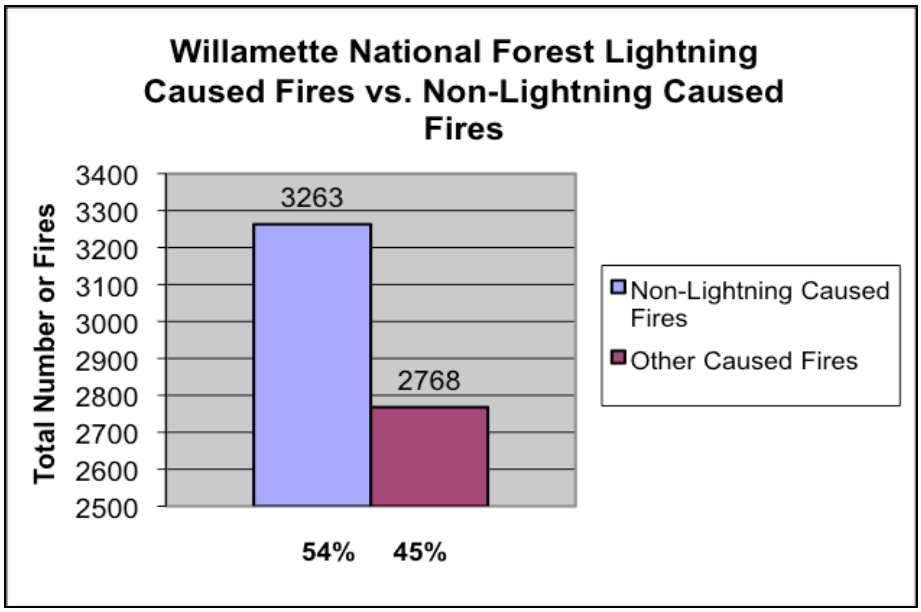

Figure 7: Histogram of both lightning-caused and non lightning-caused fires on the Willamette National Forest from 1940-2005

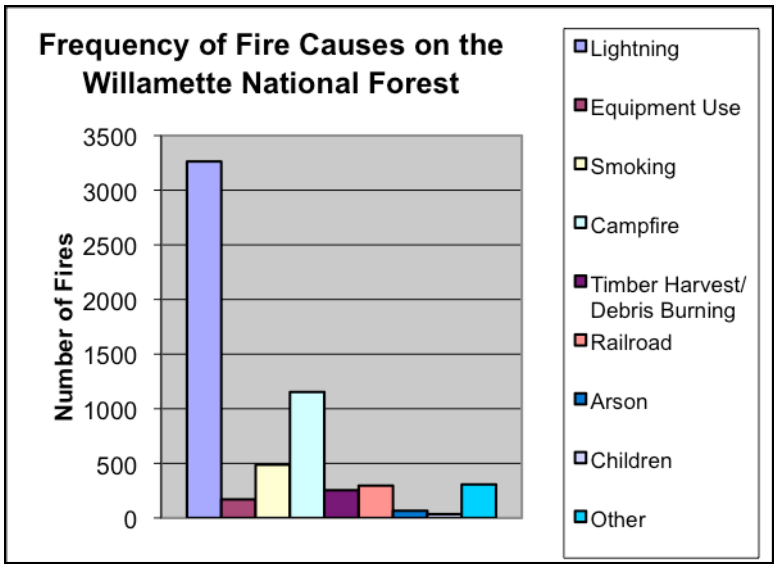

Figure 8: Frequency of fire causes on the Willamette National Forest (1940-2005).

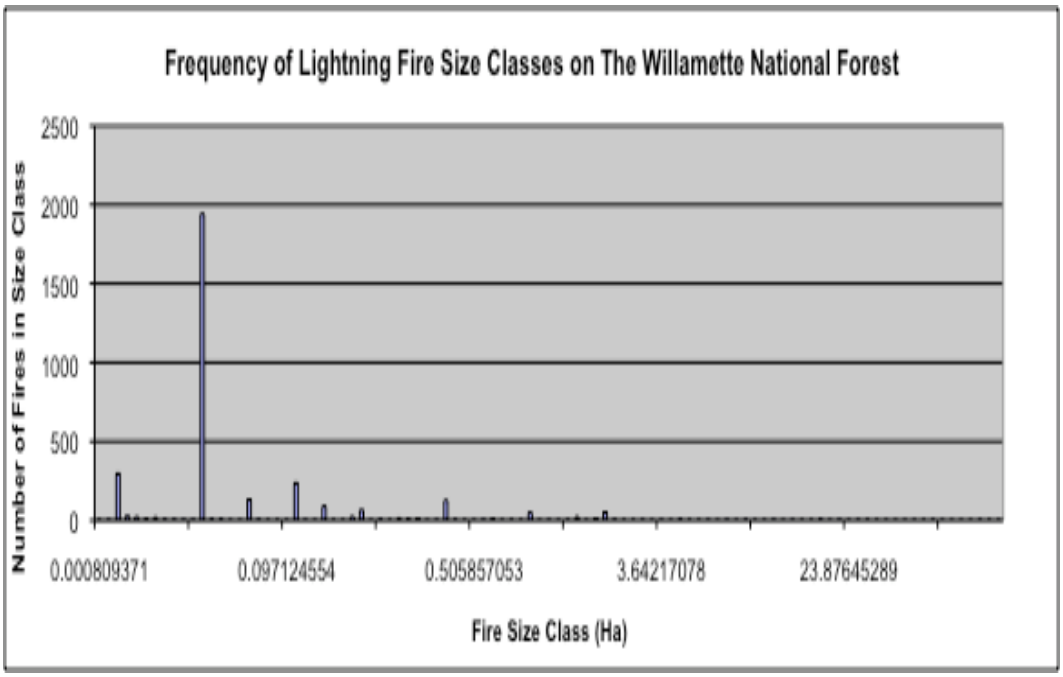

Figure 9: Frequency distribution of lightning fire size-classes on the Willamette National Forest ignited from 1940-2005.

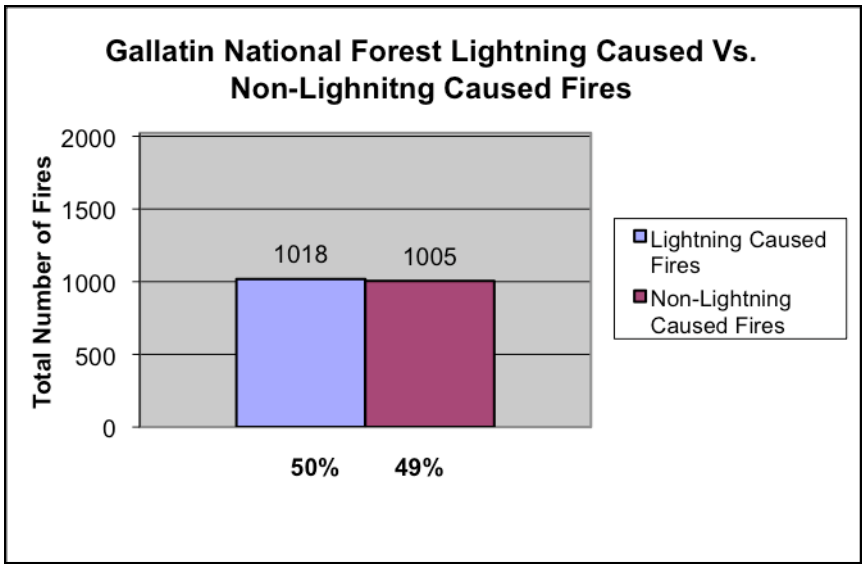

Figure 10: Histogram of both lightning-caused and non lightning-caused fires on the Gallatin National Forest from 1940-2005.

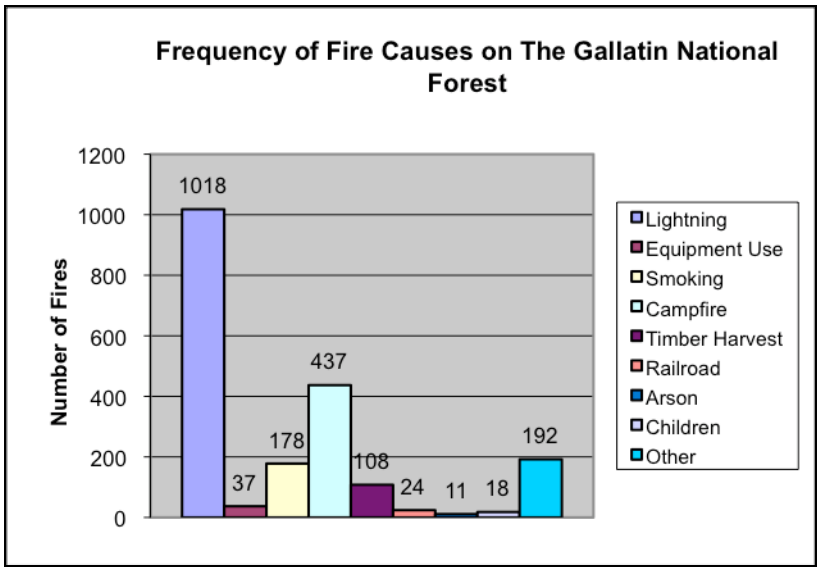

Figure 11: Frequency of fire causes on the Gallatin National Forest (1940-2005).

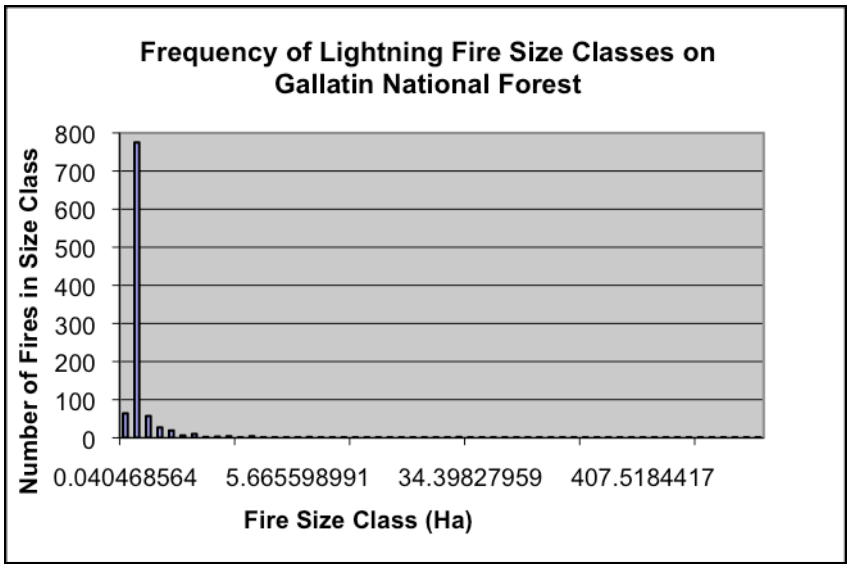

Figure 12: Frequency distribution of lightning fire size-classes on the Gallatin National Forest ignited from 1940-2005.

Probability of Lightning Caused Fires

A GLM was used to model the probability of observing a lightning fire as a function of elevation. The estimated probability density functions (pdf) of the thresholds of elevation are displayed in Figures 13 and 15. On the Willamette National Forest, elevations between 700 m and 1600 m had the highest probability of a lightning fire. The probability increased from approximately 700 m, decreases a smaller portion, then continued to increase to a peak at 1600m in a nearly bimodal pattern (Figure 13). The Gallatin National Forest had a narrower band of high probability elevations. Elevations of approximately 2300m to 2600m had the highest probability of a lightning fire. The probabilities fall off steeply on both sides of this narrow elevational band. The fitted models of both forests were used to generate a GIS layer of the probability of observing lightning-caused fires (Figures 17, 18).

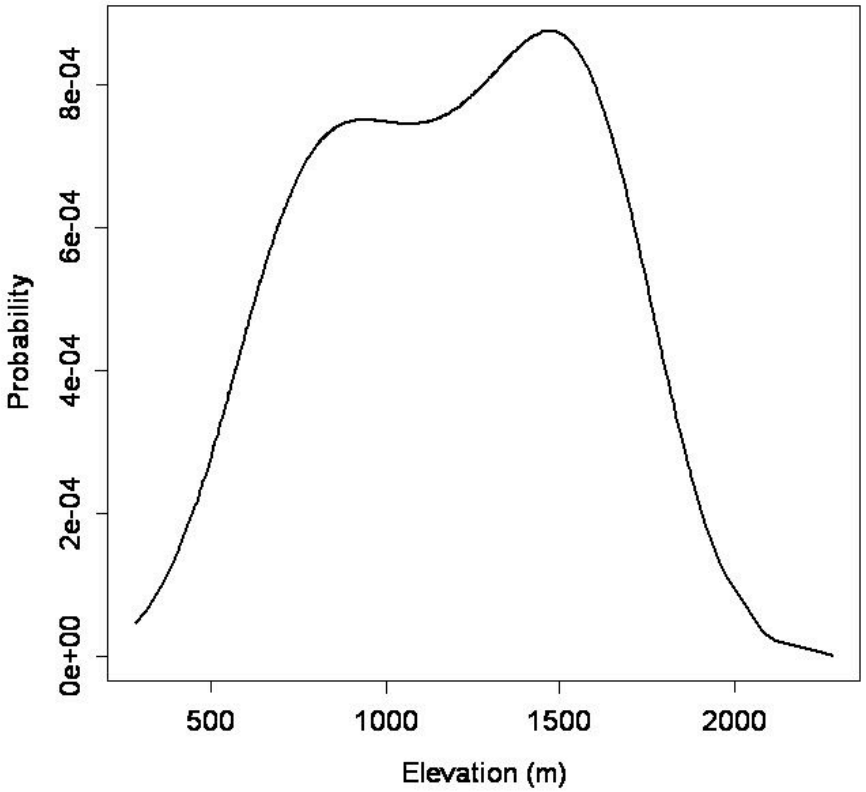

Figure 13: Willamette National Forest predicted probability density function of lightning-caused fires as a function of elevation (m).

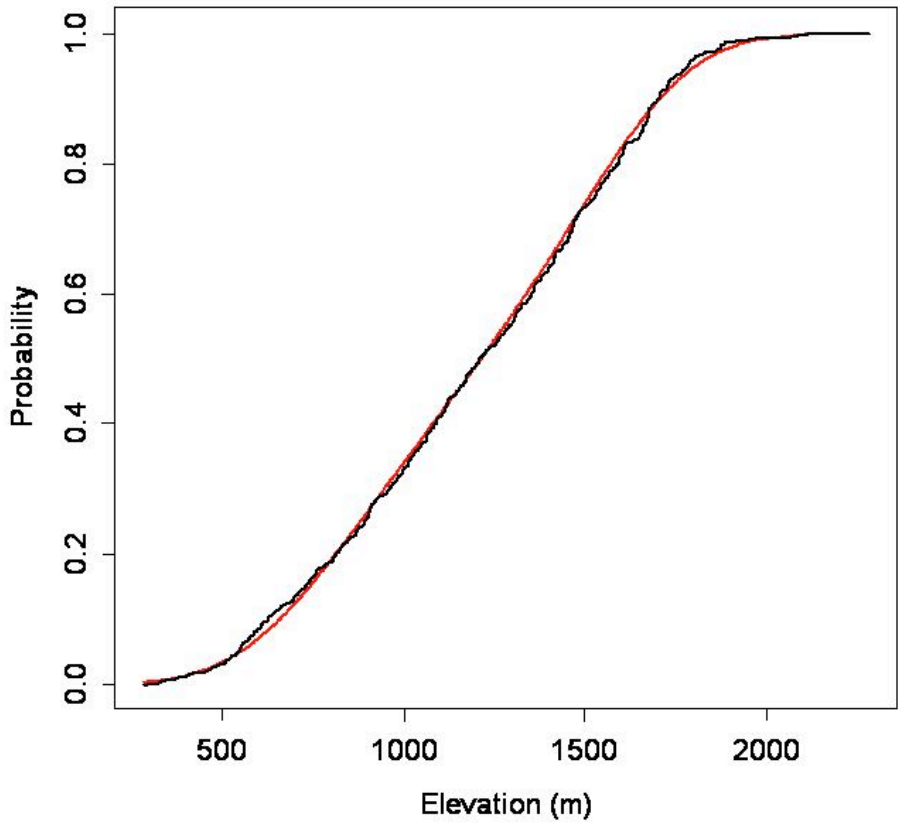

Figure 14: Observed (black line) and predicted (red line) empirical distribution function of lightning-caused fires as a function of elevation (m) on the Willamette National Forest.

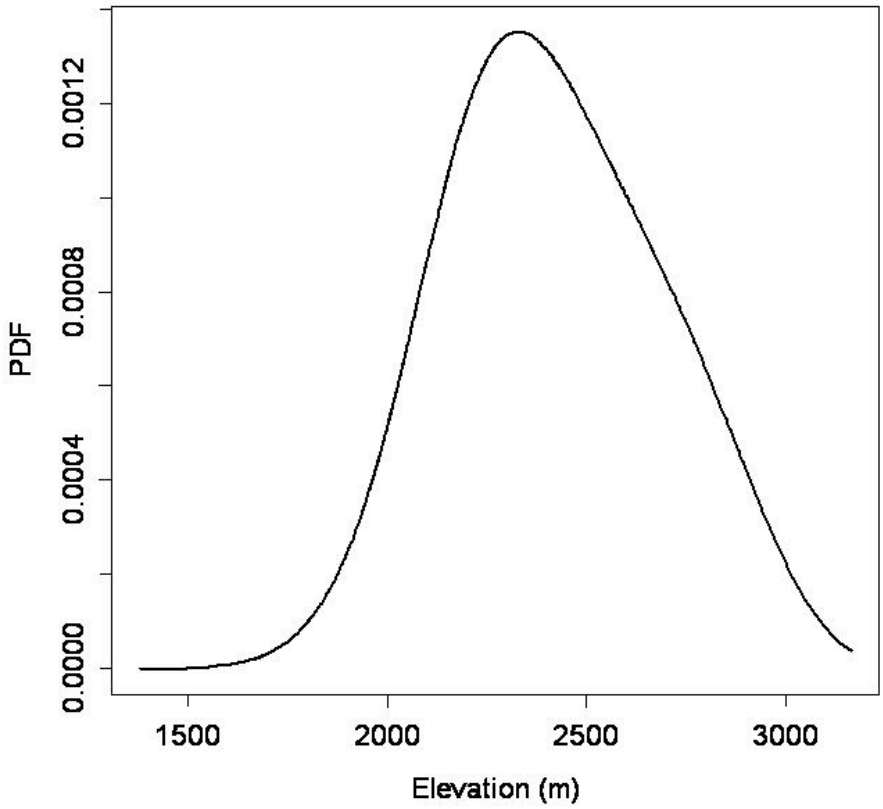

Figure 15: Gallatin National Forest predicted probability density function of lightning-caused fires as a function of elevation (m).

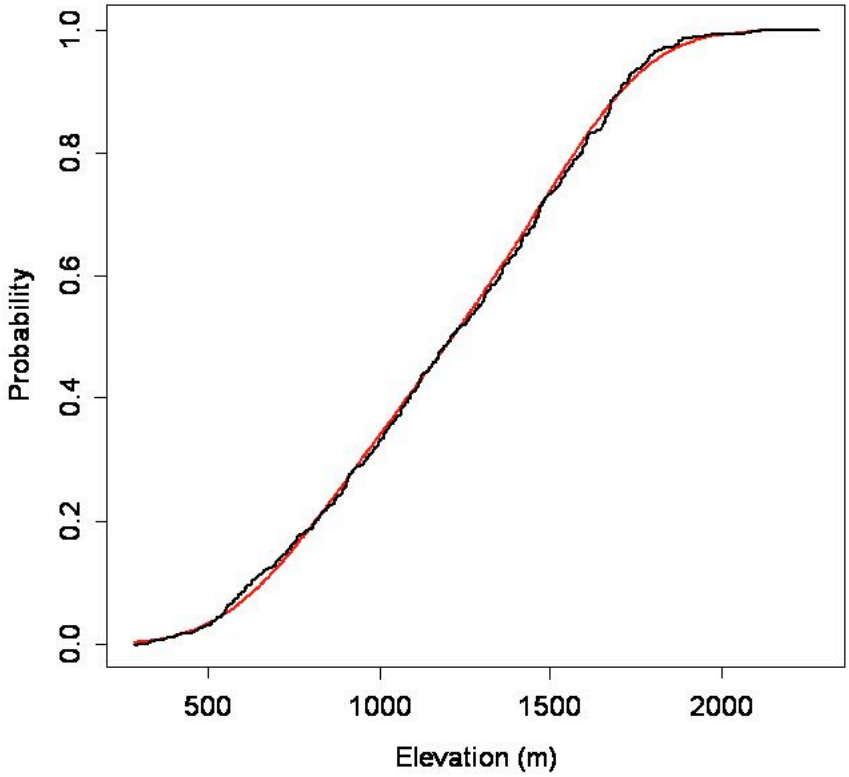

Figure 16: Observed (black line) and predicted (red line) empirical distribution function of lightning-caused fires as a function of elevation (m) on the Gallatin National Forest.

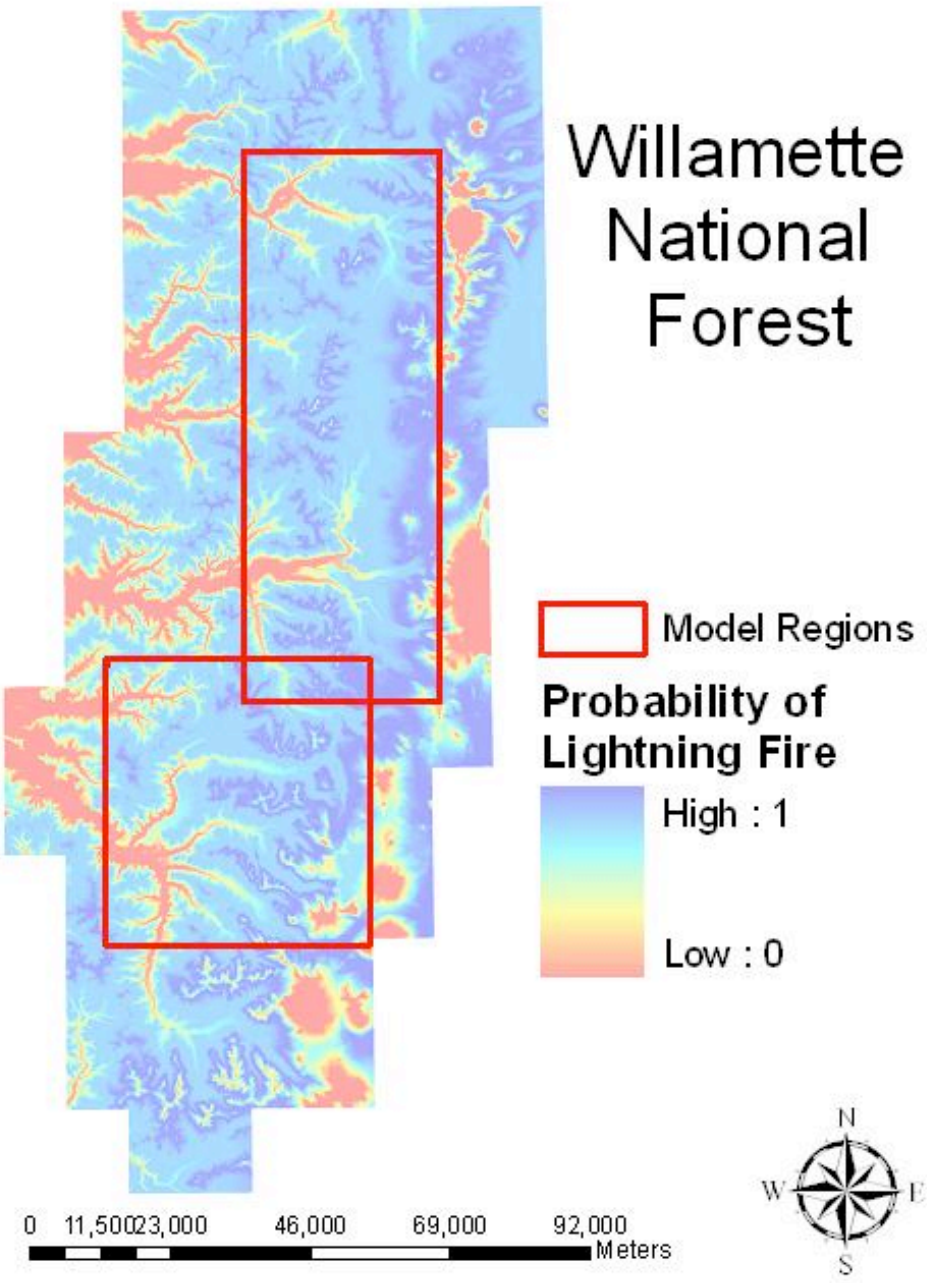

Figure 17: Distribution of the probability $p(x)/p_{max}$) of lightning caused fires on the Willamette National Forest.

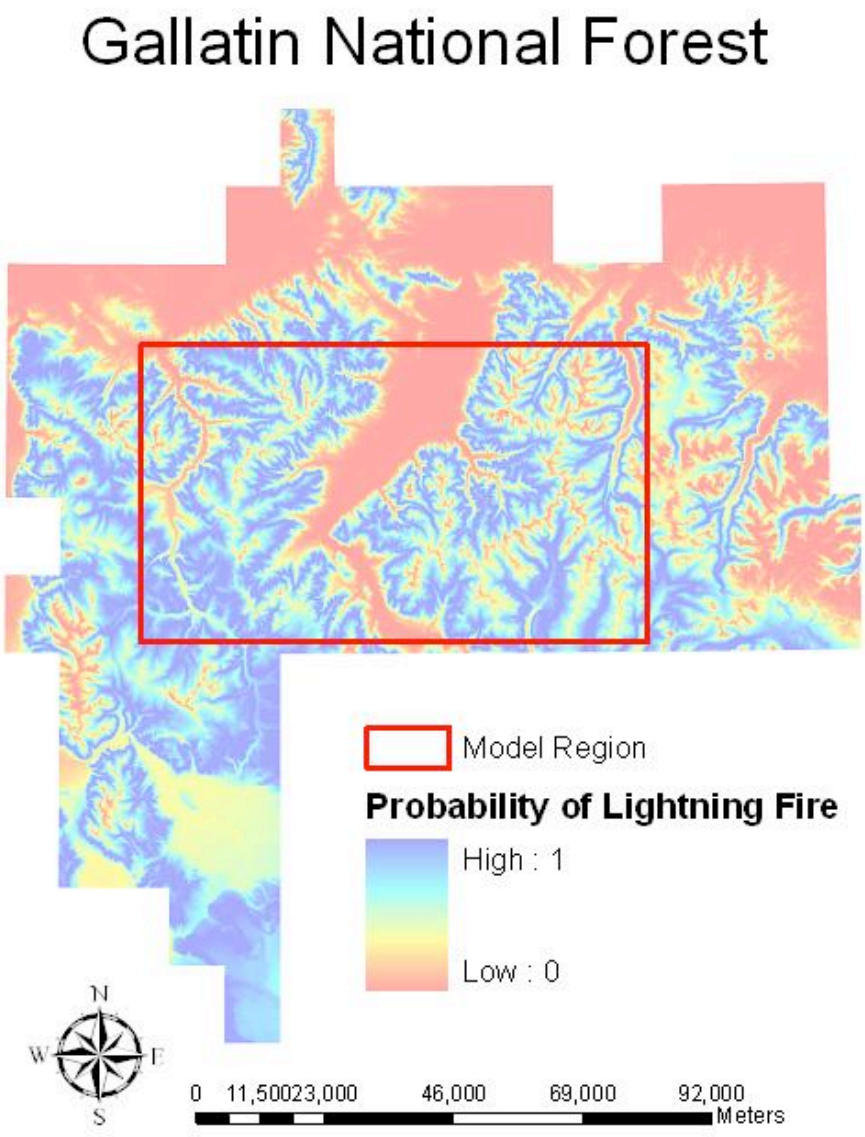

Figure 18: Distribution of the probability $p(x)/p_{max}$) of lightning-caused fires on the Gallatin National Forest.

Spatial Distribution of Lightning-Caused Fires

Willamette (Northern Modeling Region)

Figure 19 displays the transformed k-function used to test the spatial models. The black step function represents the transformed empirical k-function, while the colored lines represent the lower and upper simulation envelopes under the assumption that lightning-caused fires follow a) a Poisson distribution (red); b) inhomogenous Poisson process (blue) (i.e., elevation) and c) inhomogenous Poisson cluster process (green) (i.e., elevation plus clustering). The transformed empirical k-function extends above the simulation envelopes indicating that lightning caused fires are not randomly distributed. The Cramér-von Mises goodness-of-fit statistic also indicated non-randomness in the spatial distribution of lightning caused fires (Table 3). The p-value associated with this test was < 0.01 for all distances greater than 0.5 km. The transformed empirical k-function for the on inhomogeneous point process model that describes the spatial distribution of lightning caused fires with elevation did not account for all of the clustering associated with lightning caused fires. Elevation alone accounted for only 66% of the spatial distribution of lightning fires (Table 3). Assuming a probability of aggregation .024, with an average of 10.51 fires per cluster and a cluster radius of 2.0 *km* the transformed k-function is contained nearly perfectly within the simulation envelope, suggesting a good fit to the data. The model described 90% of the spatial distribution of lightning fires (Table 3).

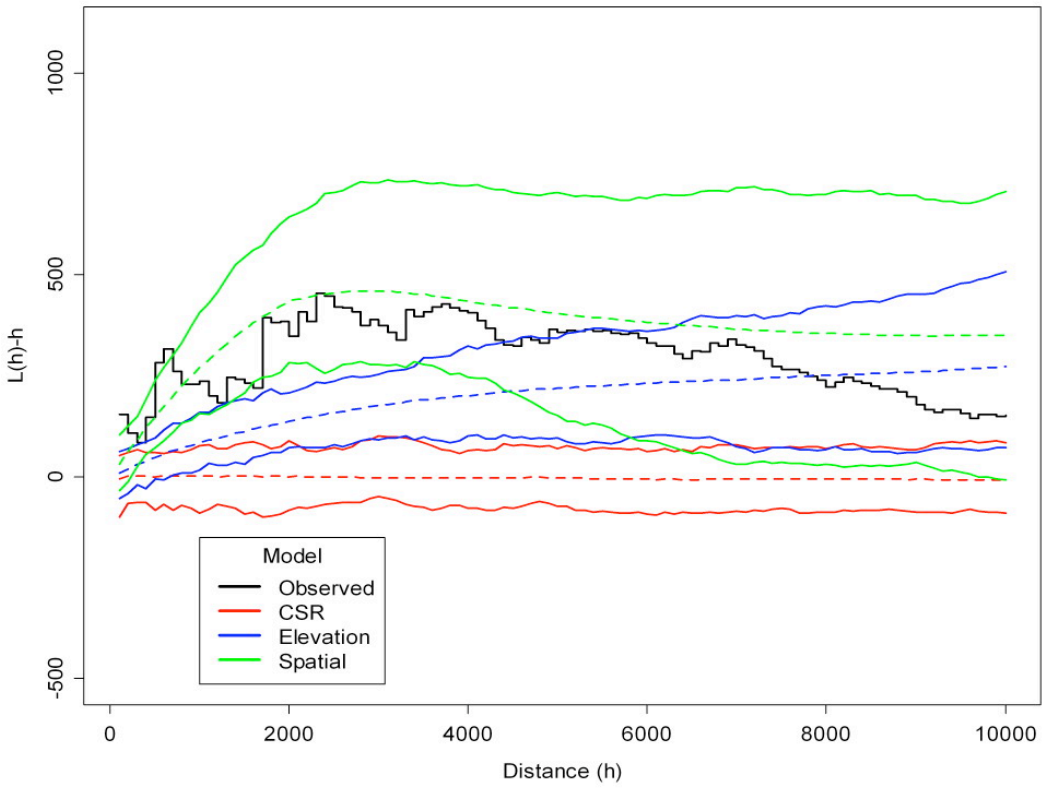

Figure 19: Plot of the transformed k-function, $L(h)=\{K(h)/\pi\}_{1/2}$ to model the spatial distribution of lightning-caused fires in the northern rectangular sub-region on the Willamette National Forest. The stair-step line represents the empirical k-function, calculated from the data. Continuous lines represent the upper and lower 99% simulation envelopes for 200 realizations of an inhomogeneous Poisson process.

Table 2: Model parameters for the Neyman-Scott point process model used to describe clustering of lightning caused fires on the Willamette and Gallatin National Forests.

National Forest	Probability of Aggregation	Cluster Size (No. Fires)	Cluster Radius (km)
Willamette			
North	0.024	10.51	2.0
South	0.024	10.51	5.0
Gallatin	0.213	10.51	5.0

Table 3: Sum of squared deviance (D) and proportion change in deviance (ΔD) based on the Cramer von Mises goodness-of-fit-statistic (Appendix B).

	National Forest					
	Willamette-North		Willamette-South		Gallatin	
Model	D	ΔD	D	ΔD	D	ΔD
CSR	1390.2	----	1008.6	----	4795.2	----
Elevation	478.1	0.66	223.5	0.78	2285.2	0.52
Spatial	135.5	0.90	130.6	0.87	679.8	0.86

Willamette (Southern Modeling Region)

Figure 20 depicts the transformed k-function used to test the goodness-of-fit of the various models in the rectangular southern region on the Willamette, and the observed (black line) and predicted (red line) empirical distribution function of lightning caused fires as a function of elevation (m) on the Gallatin National Forest.

Lightning-caused fires are not random. The Cramér-von Mises goodness-of-fit statistic also indicated non-randomness in the spatial distribution of lightning caused fires (Table 3). The p-value associated with this test was < 0.01 for all distances greater than 0.5 km. The transformed empirical k-function for the inhomogeneous point process model that describes the spatial distribution of lightning caused fires with elevation accounts for a significant proportion of the clustering of fires on the forest (78%) (Table 3). The empirical k-function was within the simulation envelope across nearly every distance. When examining the model encompassing elevation and clustering, the k-function is contained nearly perfectly within the simulation envelope, suggesting a good fit to the data for both elevation and clustering. Parameter estimates used to model the clustering included a probability of aggregation of .024, with an average of 10.51fires per cluster and a cluster radius of 5.0 *km* (Table1). The model explained 87% of the spatial distribution of lighting caused fires (Table 3).

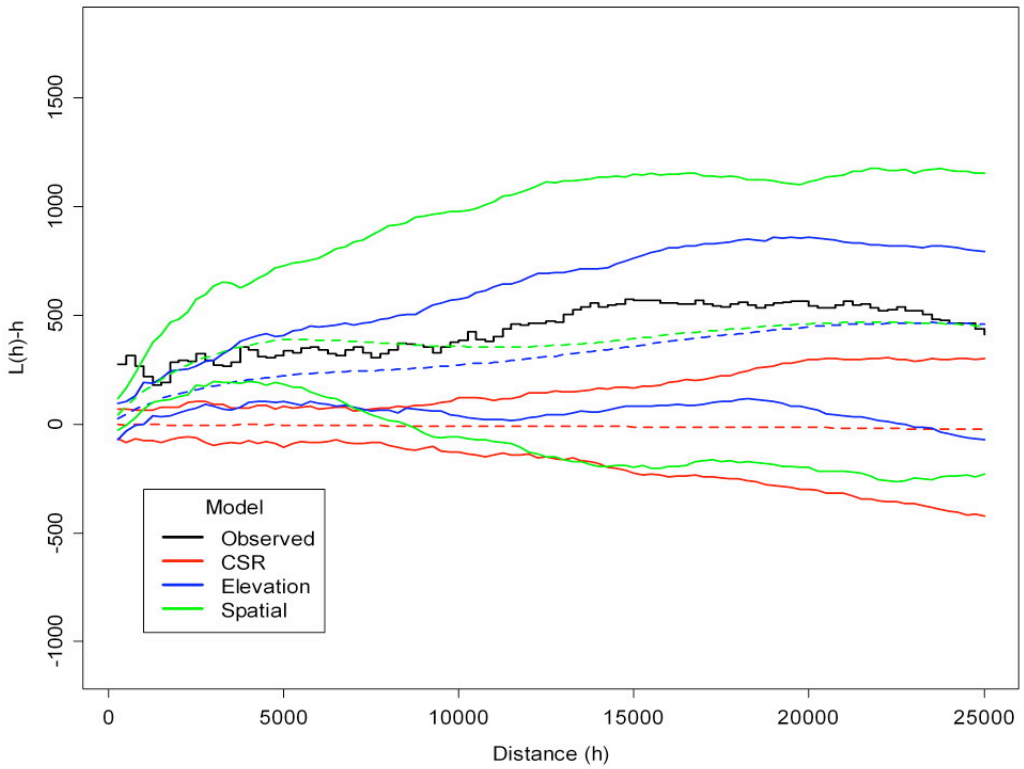

Figure 20: Plot of the transformed k-function, $L(h)=\{K(h)/\pi\}_{1/2}$ to model the spatial distribution of lightning-caused fires in the southern rectangular sub-region on the Willamette National Forest. The stair-step line represents the empirical k-function, calculated from the data. Continuous lines represent the upper and lower 99% simulation envelopes for 150 realizations of a point process model while the dashed lines represent the average value.

Gallatin

Figure 21 depicts the transformed k-function used to test the goodness-of-fit of the various models in the modeling region on the Gallatin. The observed (black line) and predicted (red line) empirical distribution function of lightning-caused fires are shown as a function of elevation (m) on the Gallatin National Forest.

Lightning-caused fires on the Gallatin, like on the Willamette, are also not random as the Cramér-von Mises goodness-of-fit statistic indicates (Table 3). The p-value associated with this test was < 0.01 for all distances greater than 0.5 km. The transformed empirical k-function for the model describing the spatial distribution of lightning fires with elevation does not account for the distribution of fires until a distance of approximately 12,500 (h) is reached, as the empirical k-function extends above the upper simulation envelope. Elevation alone accounted for only 52% of the clustering of fires (Table 3). When the model was run with elevation and clustering, the k-function is contained nearly perfectly within the simulation envelope, suggesting a good fit. The clustering was modeled assuming a probability of aggregation .213, with an average of 10.51fires per cluster and a cluster radius of 5.0 *km* (Table 2). The final model described 86% of the spatial distribution of lightning fires (Table 3).

Clustering of Fires

To describe the spatial distribution of lightning-caused fires it was necessary to assume some type of clustering. On the Willamette National Forest the probability of aggregation was 0.024, while on the Gallatin National Forest this probability was 0.21. Clusters were

randomly distributed. It was not possible to determine the exact nature of this clustering. Some clustering was due to multiple fires during a single storm event, while others were due to chance. The closest distance between any two fires was 8 m, however the time period between events was 10 years. The size of the fires may also influence this clustering. Since the majority of fires are less than 5 ha in size, there are adequate fuels available in close proximity for another fire to start. If the fires were larger, this would increase the minimum distance between fires, thus reducing the degree of clustering observed on the forests. No information was available on the forest types or fuel loading over time to evaluate the influence they may have had on the clustering.

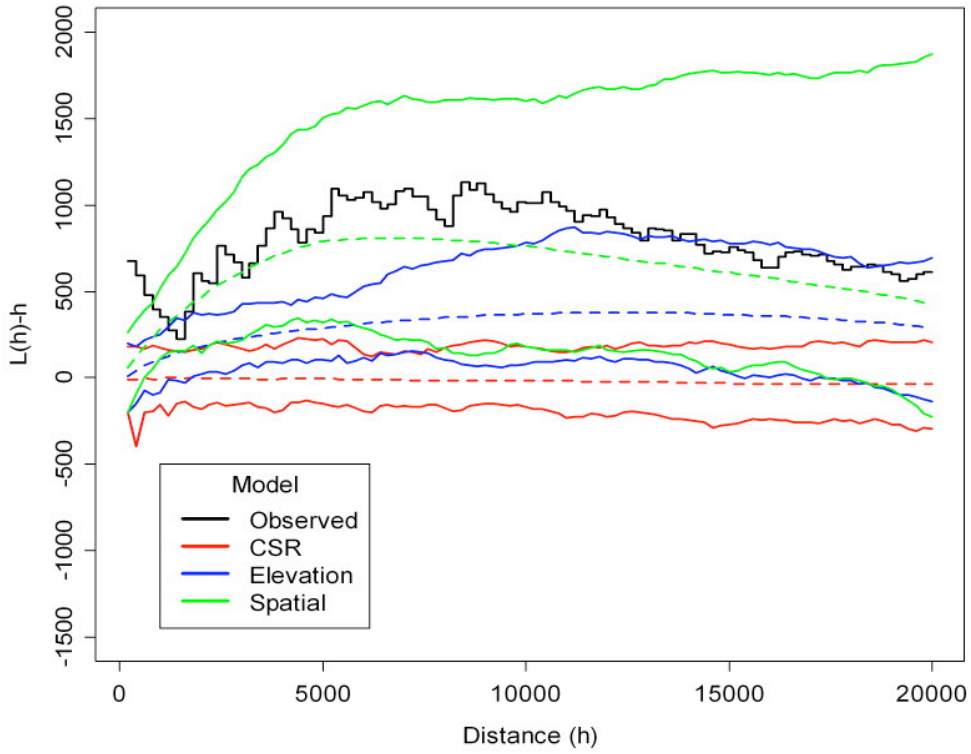

Figure 21: Plot of the transformed k-function, $L(h)=\{K(h)/\pi\}_{1/2}$ to model the spatial distribution of lightning-caused fires in the rectangular sub-region on the Gallatin National Forest. The stair-step line represents the empirical k-function, calculated from the data. Continuous lines represent the upper and lower 99% simulation envelopes for 150 realizations of a point process while the dashed lines represent the average value.

DISCUSSION

The question fire and forest managers often ask is: "Where will the next 'big one' be?" We have demonstrated that lightning fires in two divergent ecosystems share a unique spatial pattern, and can be modeled utilizing elevation as a predictor of fire distribution. On the wetter, mixed-conifer dominated Willamette National Forest, elevations most susceptible to ignition by lightning are from 700m to 1600m. On the Gallatin, the range from 2300m to 2600m is the region in which it is most probable for a fire to ignite. High fire frequencies at mid-level elevations on each forest are commonly reported in the literature (Marsden, 1982; Granstrom 1993; Barton ,1994).

These two forest types fall into unique fire regime categories. The Willamette typically undergoes more frequent, stand-replacing fires, while the Gallatin sees fewer, but often larger, stand-replacing events (Shoennagle et.al, 2004). The number and size of fires over the 65 year study period further demonstrates these differing fire regimes (Figures 7, 9,10, 12). This difference in forest type and fire regime does not detour from successfully modeling the spatial distribution of lightning fires using a parsimonious inhomogeneous Poisson cluster process. The modeling we have used is an easily repeatable standardized process for developing ignition probability surfaces with relatively easily obtainable geospatial, lightning fire, and topographic data.

Our modeled results suggest that elevation is indeed key in determining fire ignition probability. Elevations where fire frequencies are highest are often characterized by dry conditions and have fuels continuous enough to facilitate fire ignition and spread.

Forest fuel distributions also may partially explain why fires ignite in spatially clustered patterns. Areas located at a high probability elevation, and having fuel densities that are appropriate for a fire ignition, will certainly receive more fires overall, thus possibly explaining the clustering effect of many fire starts in one geographical location. Another potential explanation for the clustering of fires could be lighting storms. Topography often influences where cloud formation takes place, thus creating areas with higher probabilities of a lightning strike. When fuel, topography, and elevation all align on a landscape clustering of fire ignitions is possible.

Utilizing the probability surface for each forest (Figures 17, 18) managers may be able to combine this data with preexisting forest fuel maps to provide an even more robust set of high fire probability areas. Fuel mapping provides information about fuel types, and fuel density. Coupling the spatial distribution data with fuel mapping could provide target areas for fuel reduction projects, fire suppression staging, and urban interface fire protection.

These results ultimately provide a spatial tool helpful in focusing limited fuel treatment funds. Treatments are often prescribed in areas of high fire probability and intensity, in hopes of reducing the potential for catastrophic fire. Fire suppression resources often benefit from these reduction projects, as they can more effectively contain unwanted high intensity fire events when fuel breaks are in place.

Suppression crews must make the decision of where to stage themselves prior to a lightning event. When combined with other information such as live-time lightning maps, the analysis derived in this paper has the potential to enable managers to more effectively position personnel for quick suppression of fire starts. By suppressing fires quickly, while they are small, crews can often eliminate large catastrophic fires.

These data could also be useful in creating more accurate Wild Fire Use (WFU) maps in areas devoid of urban interface challenges. By knowing the estimated probability of a lightning fire igniting in a given area, managers may feel comfortable enough to let certain fires burn with minimal suppression. This technique not only restores natural fire to the landscape, but can also be useful in eliminating parasite infections or outbreaks in some forest types.

The most costly, and perhaps most publicized, fires are those burning in the urban interface. Millions of dollars are spent each year protecting structures (NIFC, 2008). By strategically positioning fuels reduction projects and fire suppression crews, urban interface issues can be drastically reduced. In combination with other mapping, tactical fire tools, models, and informed management decisions, these data and resources provide a platform for better forest and fire management. Ultimately, knowledge about where a fire is likely to start will save federal dollars spent on fuel reduction and suppression.

SUMMARY

By understanding the spatial distribution of lightning fires, fire and timber managers can gain a better understanding of how to spatially locate, and manage fuel treatments on these two forests. Elevation plays a significant role in the probability of a lightning strike igniting a forest fire given acceptable climatic and fuel conditions. The results of this study provide suggested ranges in elevation in which managers of these two forests, as well as managers of similar forest types, can focus attention for both fuel reduction efforts as well as urban interface fire suppression efforts.

REFERENCES

Akaike, H., 1973. Information theory and extension of the maximum likelihood principle. Pages 268-281. In: N. Petrov and F. Csaki, editors. Second International Symposioum on Information Theory. Hungarian Academy Sciences, Budapest, Hungary. Reprinted 1992 in Breakthroughs in Statistics, S. Kotz and N. Johnson, editors, 1:610-624, Springer Verlag, New York, New York, USA.

Arno S.F., Gruell G.E. 1983. Fire history of the forest-grassland ecotone in southwestern Montana. Journal of Range Management. 36: 33, 332.

Barrett S.W. 1994. Fire regimes on andesitic mountain terrain in northeastern Yellowstone National Park, Wyoming. International Journal of Wildland Fire 4(2):65-76.

Besag, J.E., Diggle, P.J., 1977. Simple Monte Carlo tests for spatial patterns. Applied Stat. 26, 327-333.

Borig, M.L., Feguson, S.A., 2002. The 2000 fire season: Lightning-caused fires. J. Applied Meterology. 41, 786.79.

Breiman, L., Friedman, J., Olshen, R., & Stone, C. (1984). "Classification and Regression Trees," Wadsworth.

Cressie, N., 1991. Statistics for spatial data. John Wiley and Sons, New York.

Fisher W.C., Clayton B.D. 1983. Fire ecology of Montana forest habitat types east of the continental divide. NTIS, Springfield, VA (USA).

Granstom, A., 1993. Spatial and temporal variation in lightning ignition in Sweden. Journal of Vegetation Science 4, 737-744.

Harrell, F.E., 2001. Regression modeling strategies with application to linear models, logistic regression, and survival analysis. Springer Series in Statistics, Springer, New York. 568 p.

Keane R.E., Arno S.F. 1993. Rapid decline of whitebark pine in western Montana: evidence from 20-year re-measurements. Western Journal of Applied Forestry 8(2):44-47.

Larjauaara, M., Kuuluvainen, T., Rita, H., 2005. Spatial distribution of lightning-ignited forest fires in Finland. For. Ecol. & Management 208, 177-188.

Lewis, P.A.W., Shodler,G.S., 1979. Simulation of a non-homogeneous Poisson process by thinning. Naval Research Logistic Quarterly. 26, 403-413.

Losensky B.J.. 1993. Historical vegetation in region one by climatic area. On file at Lolo National Forest, Fire Management Office, Missoula, MT.

Marsden, M., 1982. A statistical analysis of the frequency of lightning-caused forest fires. Journal of Environmental Management 14, 149-159.

Moore M, M, Covington W.W, Fuel PZ. 1999. Reference conditions and ecological restoration: A southwestern ponderosa pine perspective. Ecological Applications 9:1266.

Morgan P., Bunting S.C., Keane R.E., Arno S. F. Fire ecology of whitebark pine forests of the northern Rocky Mountains, USA. Proceedings in International Workshop on Subalpine Store. United States Department of Agriculture Forest Service Rocky Mountain Research Station General Technical Report: RMRS-GTR-42 Vol. 2.

National Interagency fire Center. 2008. www.nifc.gov.

National Oceanic and Atmospheric Administration. 2006. www.noaa.gov.

Neter, J., Wasserman, W., Kutner, M.H., 1985. Applied linear models, regression, analysis of variance, and experimental designs. Irwin, Homeland, Ill. 1127 p.

Podur, J. 2003. Spatial patterns of lightning-caused forest fires in Ontario, 1976-1998. Ecological Modelling. 164, 1-20.

Podur, J., Martell, D.I., Csillag. F., 2003. Spatial patterns of lightning-caused forest fires in Ontario. Ecol. Model. 164, 1-20.

R: A Language and Environment for Statistical Computing, R Development Core Team, R Foundation for Statistical Computing, Vienna, Austria, 2005, http://www.R-project.org.

Ripley, B.D., 1977. Modeling spatial patterns. J. Royal Stat. Soc., Series B 39, 172-192.

Shoennagel T., Veblen T.T, Romme W.H., 2004. The interaction of fire, fuels, and climate across rocky mountain forests. Bioscience 54, 7 pg 661.

Tomback D.F., Hoffman L.A., Sund S. 1990. Coevolution of whitebark pine and nutcrackers: Implications for forest regeneration. In: Proceedings of the symposium: whitebark pine ecosystems: Ecology and management of a high mountain resource, March 29-31, 1989, Bozeman, MT. Gen. Tech. Rep. INT-270. Ogden, UT: US. Department of Agriculture, Forest Service, Intermountain Research Station: 118-130.

USDA Department of Agriculture. 2002. A collaborative Approach for Reducing Wildland Fire Risks to Communities and the Environment: 10-year Comprehensive strategy. (18 June 2004; www.fireplan.gov/reports/7-19en.pdf)

USDA Forest Service. 20068. Gallatin National Forest Website. http://www.fs.fed.us/r1/gallatin/.

USDA Forest Service. 2008. Willamette National Forest Website. http://www.fs.fed.us/r6/willamette/.

Veblen T.T. Kitzberger T, Donnegan J. 2000. Climatic and human influences on fire regimes in ponderosa pine forests in the Colorado Front Range. Ecological Applications 10:1178-1195.

APPENDIX

Appendix A: Logit models for creation of cdf 's

Willamette logit model is:

$$y = -10.042 + 0.0196*E - 1.435\times10^{-5}*E^2 + 4.149\times10^{-9}*E^3$$

$$(0.10)\quad (2.88\times10^{-4})\quad (2.56\times10^{-7})\quad (7.12\times10^{-11})$$

$$s_{xy} = 0.161, \quad n=679, \quad R^2 = 0.992$$

*The numbers in parentheses are the standard errors of the regression coefficients.

Gallatin logit model is

$$y = -88.342 + 0.126*E - 8.841814\times10^{-05}*E^2 + 3.837\times10^{-8}*E^3$$
$$(20.14)\quad (4.64\times10^{-2})\quad (4.22\times10^{-5})\quad (1.90\times10^{-7})$$

$$- 9.527\times10^{-12}*E^4 + 1.007845\times10^{-15}*E^5$$
$$(4.21\times10^{-12})\quad (3.69\times10^{-16})$$

$$s_{xy} = 0.144, \quad n=798, \quad R^2 = 0.997$$

*The numbers in parentheses are the standard errors of the regression coefficients.

Appendix B: Goodness-of-fit equation:

$$D = \sum_{l=1}^{h0} \left(\hat{K}(h)^{0.25} - \overline{K}(\theta; h)^{0.25} \right)^2$$

where $\hat{K}(h)$ is the empirical k-function (observed), and $\overline{K}(\theta; h)$ is the hypothesized k-function with parameters θ.

Proportion change in the goodness-of-fit statistics

$\Delta D=(D_R - D_j)/D_R$
D_R = D for CSR

D_j = D for elevation or spatial model